DALTON
FULL PAPER

A kinetic study of the redox behaviour of Fe^{III}(TPPS) [TPPS = 5,10,15,20-tetrakis(*p*-sulfonato)porphyrinate] in the presence of peroxomonosulfate, hydrogen peroxide, and sulfite/oxygen. Direct evidence for multiple redox cycling and suggested mechanisms †

Vasilios Lepentsiotis,[a] Rudi van Eldik,*[a] Frans F. Prinsloo[b] and Jakobus J. Pienaar*[b]

[a] *Institute for Inorganic Chemistry, University of Erlangen-Nürnberg, Egerlandstr. 1, 91058 Erlangen, Germany*
[b] *Atmospheric Chemistry Research Group, Department of Chemistry, Potchefstroom University, Potchefstroom 2520, South Africa*

Received 7th April 1999, Accepted 18th June 1999

The reactions of the water soluble complex Fe^{III}(TPPS) [TPPS = 5,10,15,20-tetrakis(*p*-sulfonatophenyl)porphyrinate] with peroxomonosulfate, hydrogen peroxide and sulfite/oxygen have been investigated kinetically as a function of reactant concentration and pH. The spectral changes recorded for the reactions between the Fe^{III}(TPPS) dimer and peroxomonosulfate and hydrogen peroxide can be interpreted in terms of a redox cycle between (TPPS)$Fe^{III}OFe^{III}$-(TPPS) and (TPPS)$Fe^{III}OFe^{IV}$(O)(TPPS$^+$), and in terms of multiple redox cycles also involving Fe^{II}(TPPS) for the Fe^{III}(TPPS)–sulfite–oxygen system. In the case of peroxomonosulfate and hydrogen peroxide a slow redox cycle (1000 s) between iron-(III) and -(IV) complexes is observed at low [SO_5^{2-}] and [H_2O_2]. In the case of sulfite–oxygen the kinetic traces are quite different; the Fe^{III}/Fe^{IV} redox cycle is very fast (a few seconds) and is only observed after what appears to be an induction period. Furthermore, it also depends significantly on the selected experimental conditions (pH, sulfite and oxygen concentration). Rapid-scan techniques were used to study these redox cycles. Reaction mechanisms for the redox cycling of the Fe^{III}(TPPS)–SO_5^{2-} system, and for the multiple redox cycling of the Fe^{III}(TPPS)–sulfite–oxygen system, are proposed. They are based on reactions that participate in the suggested mechanism for the iron-catalysed autoxidation of sulfite. In contrast to the Fe^{III}(TPPS)–HSO_5^- system, which is insensitive to oxygen, oxygen plays an essential role in the multiple redox cycles of the Fe^{III}(TPPS)–sulfite–oxygen system, which is accounted for in the proposed mechanism. Computer simulations based on the proposed reaction mechanisms are in good agreement with the observed experimental kinetic traces and indicate that for the Fe^{III}(TPPS)–sulfite–oxygen system the formation of the $SO_5^{\bullet -}$ radical is the main oxygen-consuming step during the overall redox process.

Introduction

In the past metalloporphyrins have been extensively investigated[1] mainly because of their relevance to biological systems. More recently there is also a great interest in oxidation reactions involving metalloporphyrins[2–4] since it is known that they are very versatile oxidation catalysts for many different reactions, *e.g.* sulfite oxidation, olefin epoxidation, alkane hydroxylation, pollutant oxidation, drug metabolization and DNA cleavage.

In environmental processes the metal-catalysed oxidation of sulfur(IV) oxides plays an important role in atmospheric chemistry, as well as in industrial flue gas desulfurization processes.[5] It has been suggested that the iron(III) catalysed autoxidation reaction of such oxides in the atmosphere is partly responsible for the acidification of precipitation.[5] Several investigations have been undertaken in recent years in order to try to understand the catalytic role of Fe^{III} and of transition metal ions and complexes in general, during such autoxidation processes.[6–12] There is general agreement that the metal ion in its higher (usually +3) oxidation state can initiate a free radical process *via* an electron-transfer reaction (1), that leads to the formation of the

$$M^{n+} + HSO_3^- \longrightarrow M^{(n-1)+} + SO_3^{\bullet -} + H^+ \qquad (1)$$

sulfite radical. The sulfite radical ($SO_3^{\bullet -}$) can react rapidly with oxygen to form the strong oxidizing peroxomonosulfate radical ($SO_5^{\bullet -}$), eqn. (2), which can reoxidize the metal ion back to the higher oxidation state, eqn. (3).

$$SO_3^{\bullet -} + O_2 \longrightarrow SO_5^{\bullet -} \qquad (2)$$

$$M^{(n-1)+} + SO_5^{\bullet -} + H^+ \longrightarrow M^{n+} + HSO_5^- \qquad (3)$$

A redox cycling of the metal ion can thus in principle occur and a generalized reaction scheme, showing the role of one electron metal oxidants in the autoxidation of sulfite in aqueous solution, has been proposed[13] for this process. In these reaction systems $SO_5^{\bullet -}$, HSO_5^- and $SO_4^{\bullet -}$ can either reoxidize the reduced metal ion, or react with sulfite to lead to the final sulfur oxidation products.

One of the water soluble metalloporphyrins, iron(III) tetrakis-(*p*-sulfonatophenyl)porphyrinate (abbreviated Fe^{III}(TPPS)), is known to be a catalyst for the electrocatalytic reduction of HSO_3^- to H_2S[14] and for the electrocatalytic oxidation of sulfite to sulfate.[15] It is also known that metal ions (*e.g.* Co^{III}, Fe^{III}) coordinated to TPPS undergo redox reactions in the presence of

† *Supplementary data available*: absorbance spectral changes. For direct electronic access see http://www.org/suppdata/dt/1999/2759/, otherwise available from BLDSC (No. SUP 57588, 9 pp.) or the RSC Library. See Instructions for Authors, 1999, Issue 1 (http://www.rsc.org/dalton).

alcohols and on irradiation by light.[16,17] The trivalent metal ion is reduced to the divalent ion with simultaneous oxidation of alcohols and it was found that the metalloporphyrin played a photocatalytic role in the autoxidation of alcohols.[16,17] Recent studies in our laboratories have focused on the catalytic effect of Co^{III}(TPPS) and Mn^{III}(TPPS) in the autoxidation of sulfite.[18,19] In both cases redox cycling of the metalloporphyrin was observed.

Redox cycling of metal ions and complexes forms the basis of the catalytic activity of these species in the mentioned reactions. We have therefore in this study investigated the reactions between Fe^{III}(TPPS), sulfite and oxygen in aqueous solution in search of evidence for redox cycling of this metalloporphyrin by means of rapid-scan spectrophotometry. In addition, the reaction of Fe^{III}(TPPS) with other redox partners such as H_2O_2 and $KHSO_5$ was also investigated in an effort to elucidate the detailed reaction mechanism of the sulfite/oxygen system.

Experimental

Chemicals of analytical reagent grade (Merck, Fluka and Aldrich) and deionized Millipore water (18 Mohm) were used to prepare all solutions. Argon or nitrogen gas was used to deaerate solutions when required. Aqueous $HClO_4$ and NaOH were used to adjust the pH, and $NaClO_4$ to adjust the ionic strength. The complex Fe^{III}(TPPS) was synthesized according to standard literature methods[20] and the purity checked by UV-VIS spectroscopy and elemental (C,H,N) analysis.

The UV-VIS spectra were recorded on an HP 8452A diode array spectrophotometer or on a Shimadzu UV-2102/3102PC spectrophotometer. Rapid scan measurements were performed on a Bio Sequential SX-17MV Stopped-Flow Reaction Analyser from Applied Photophysics equipped with a J & M detector connected to a TIDAS 16-416 spectrophotometer. Stopped-flow measurements were performed on a Bio Sequential SX-18MV stopped flow spectrofluorimeter. Spectroelectrochemical experiments were carried out employing a Perkin-Elmer Lambda 9 spectrophotometer. Data accumulation was performed with the PECSS software package on a PC Acer 910 and an Amel 550 potentiostat/galvanostat was used. Details of the spectroelectrochemical cell are given elsewhere.[21]

Results and discussion

In acidic solutions Fe^{III}(TPPS) exists as a monomer which is deep orange-brown, whereas in basic solutions the green μ-oxo dimer is formed.[20] The equilibrium constant for formation of the dimer and the kinetics of dimerization were studied by different groups.[20,22–24] From our spectrophotometric titrations we obtained a pK_a value of 6.7 ± 0.2 (I = 0.1 M) for the monomer which is in close agreement with the literature value of 7.0 ± 0.2[24] at 25 °C.

Spectroelectrochemical experiments with Fe^{III}(TPPS) clearly show that electrochemical reduction and oxidation of it result in characteristic spectral changes (see Fig. 1, SUP 57588). In the case of reduction the Soret band of the Fe^{III}(TPPS) monomer (λ_{max} = 395 nm) decreases while a new band is being formed at longer wavelength (λ_{max} = 426 nm) and with a higher molar absorptivity. In addition, a broad weak band is also formed at 550 nm. These spectral changes are in full agreement with literature data[15,17,24] and can be assigned to the reduction of Fe^{III}(TPPS) to Fe^{II}(TPPS). When Fe^{III}(TPPS) is electrochemically oxidized the Soret band is decreased without any formation of a new band at longer wavelength (see SUP 57588) which according to the literature[25] is due to the formation of the $Fe^{III}(TPPS^+)$ radical cation. Analogous spectral changes for reduction and oxidation were also observed for the Fe^{III}(TPPS) dimer at high pH (>10). The electrochemical reduction and oxidation of Fe^{III}(TPPS) were almost fully reversible under these conditions.

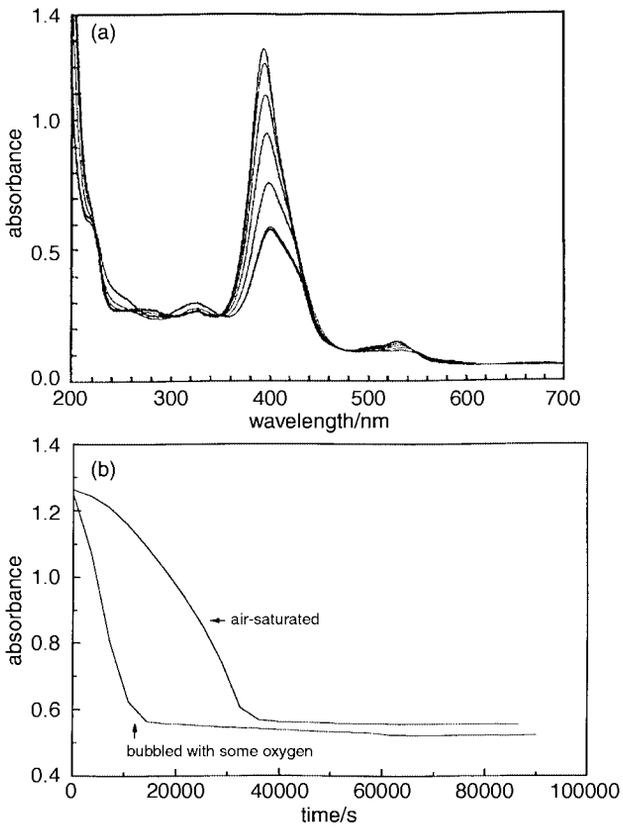

Fig. 1 (a) Spectral changes observed for the reaction between Fe^{III}(TPPS) and sulfite in air saturated solutions (Δt = 2 h). (b) Absorbance–time traces for the decomposition of Fe^{III}(TPPS) by sulfite (λ = 395 nm). Experimental conditions: $[Fe^{III}(TPPS)] = 1 \times 10^{-5}$ M; $[S^{IV}] = 1 \times 10^{-3}$ M; pH 3; T = 25 °C; I = 0.1 M.

Nearly all investigations of the Fe^{III}(TPPS) system were performed at pH 3 (monomer) and 11 (dimer) without using any buffers since these values are far away from the pK_a value associated with the dimerization. The stability of the Fe^{III}(TPPS) monomer and μ-oxo dimer was checked by UV-VIS spectroscopy showing that there was nearly no decomposition over several days.

Preliminary and qualitative observations

First, the reaction between the Fe^{III}(TPPS) monomer and sulfite was followed over a longer period of time at pH 3 using a tandem cuvette. The sulfite and oxygen concentrations were varied, whereas the Fe^{III}(TPPS) concentration (1×10^{-5} M) and the ionic strength (0.1 M) were kept constant. Fig. 1(a) shows the spectral changes observed for the reaction of Fe^{III}(TPPS) with a large excess of sulfite (1×10^{-3} M) in air-saturated solutions. The cycle time between each consecutive spectrum is 2 h. The Soret band of the Fe^{III}(TPPS) monomer decreases with time without the formation of the characteristic band for Fe^{II}(TPPS) at longer wavelength as observed electrochemically. There is, however, some peak broadening, which indicates that partial formation of Fe^{II}(TPPS) does occur. This indicates that the expected reduction of Fe^{III}(TPPS) to Fe^{II}(TPPS) is dominated by an overall decomposition of the Fe^{III}(TPPS) complex under these conditions. Absorbance–time traces indicate a typical autocatalytic behaviour for this decomposition process that strongly depends on the oxygen concentration in solution (see Fig. 1b). Surprisingly, if the sulfite concentration is increased from 1×10^{-3} to 1×10^{-2} M at constant Fe^{III}(TPPS) concentration and in air-saturated solutions, the decomposition of Fe^{III}(TPPS) is inhibited. However, a decrease in the sulfite concentration from 1×10^{-3} to 1×10^{-4} M results in the oppos-

ite effect and the decomposition of Fe^{III}(TPPS) is accelerated. These trends clearly indicate that the sulfite : oxygen concentration ratio controls the concentration of the strongly oxidizing sulfur oxide radicals that must account for the overall decomposition of the Fe^{III}(TPPS) complex, since at high sulfite concentrations competing side reactions between the sulfur oxide radicals ($SO_5^{\bullet -}$, $SO_4^{\bullet -}$, *etc.*) and sulfite occur. An increase in the oxygen concentration results in an acceleration of the Fe^{III}(TPPS) decomposition since more sulfur oxide radicals are formed. In summary, under strongly oxidizing conditions (high oxygen concentration and low sulfite concentration) the decomposition of Fe^{III}(TPPS) by sulfite is favoured.

Analogous measurements were performed at pH 11 for the reaction between the Fe^{III}(TPPS) dimer and sulfite. Under similar conditions the decomposition of the dimer (decrease of the Soret band) is observed, showing the same kind of trends as observed for the monomeric species. The decomposition of the Fe^{III}(TPPS) dimer is faster than that of the monomer. The influence of pH and of the nature of the Fe^{III}(TPPS) species has also been observed for the reaction of hydroxyl radicals with Fe^{III}(TPPS).[26] At pH 11 the rate constant was found to be much higher than at pH 7.5, which was assigned to the deprotonation of the axial ligands of Fe^{III}(TPPS) (H_2O at pH 7.5; OH^- at pH 11).[26]

These qualitative observations demonstrate that the redox behaviour of Fe^{III}(TPPS) in the presence of sulfite/oxygen is rather complex and calls for a more detailed analysis. For that reason we have first studied the redox behaviour of Fe^{III}(TPPS) in the presence of species that are relevant to the sulfite/oxygen system, in order to clarify the reported observations.

Reaction of Fe^{III}(TPPS) with $KHSO_5$

Since the peroxomonosulfate radical plays an important role in the redox cycling of metal ions[13] and leads to the formation of peroxomonosulfate (SO_5^{2-}), the reaction between Fe^{III}(TPPS) and oxone ($2KHSO_5$, $KHSO_4$, K_2SO_4) was studied in more detail. First the reaction was investigated in acidic medium (pH 3) where Fe^{III}(TPPS) exists as a monomer. In this case only decomposition of the Fe^{III}(TPPS) was observed, the rate of which increased with increasing $KHSO_5$ concentration. Different results were observed in basic medium (pH 11) where the reaction of $KHSO_5$ with the Fe^{III}(TPPS) dimer resulted in the formation of a new absorption band at 420 nm (Fig. 2a). These spectral changes do not correspond to those observed during the electrochemical reduction to Fe^{II}(TPPS), since λ_{max} is now at 420 and 525 nm. In addition, the absorbance changes are much smaller, indicating that in the case of the reaction with $KHSO_5$ another Fe(TPPS) species must be formed. This assumption is supported by the fact that in the same pH range the use of reducing agents such as ascorbate and dithionite did indeed lead to the formation of the Fe^{II}(TPPS) band at 426 nm with a much higher molar absorptivity. We conclude that the spectral changes observed in Fig. 2(a) must be due to the formation of an $Fe^{IV}(O)(TPPS^+)$ species at pH 3 or $(TPPS)Fe^{III}OFe^{IV}(O)(TPPS^+)$ at pH 11 since $KHSO_5$ is a strong oxidizing agent ($E^\circ = 1.82$ V[27]). Further support for this suggestion came from experiments with hydrogen peroxide (H_2O_2) as reported in the following subsection.

Following the formation of the band at 420 nm, decomposition of $(TPPS)Fe^{III}OFe^{IV}(O)(TPPS^+)$ immediately occurs (Fig. 2b). If the $KHSO_5$ concentration is decreased from 4×10^{-3} to 2.5×10^{-5} M, both the formation of the band at 420 nm and the subsequent decomposition are significantly slower. A further decrease in the $KHSO_5$ concentration (from 2.5×10^{-5} to 3×10^{-6} M) to nearly the equivalent amount of Fe^{III}(TPPS) (monomer concentration 6×10^{-6} M) resulted in a redox cycle (Fig. 2c). In the case of $KHSO_5$ it is necessary to work at very low concentrations, since its strong oxidizing property can cause the overall decomposition of the complex.

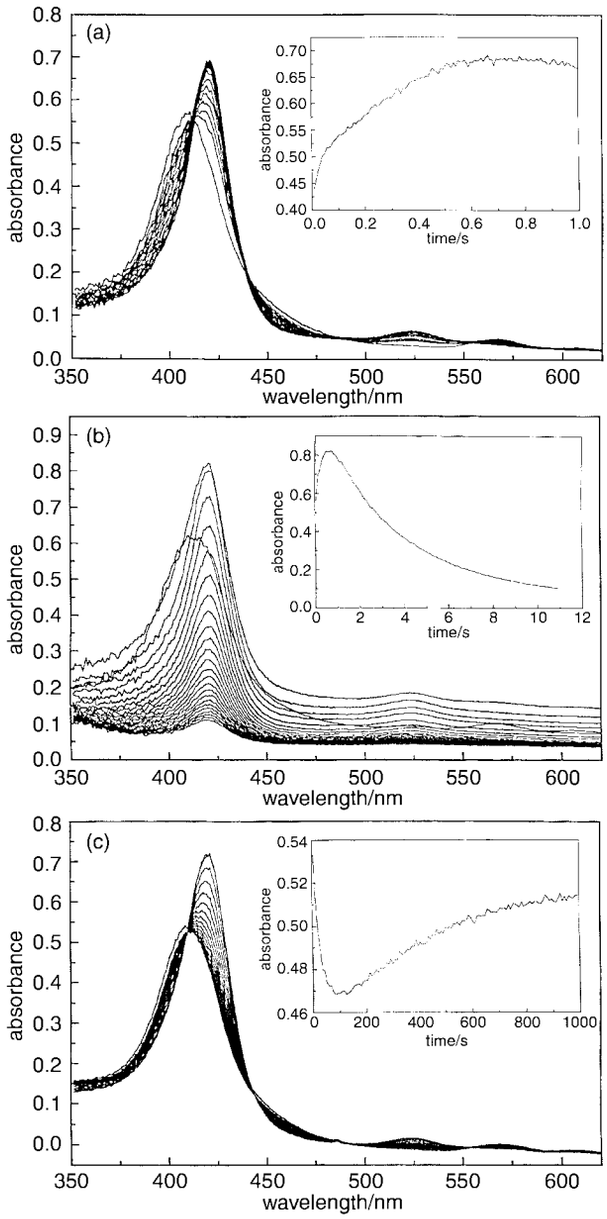

Fig. 2 Spectral changes observed for the reaction between the Fe^{III}(TPPS) dimer and $KHSO_5$ in air saturated solutions. Insert: absorbance *vs.* time at the listed wavelength. (a) $\Delta t = 0.06$ s; $\lambda = 421$ nm; $[KHSO_5] = 8 \times 10^{-3}$ M. (b) $\Delta t = 0.44$ s; $\lambda = 421$ nm; $[KHSO_5] = 6 \times 10^{-3}$ M. (c) $\Delta t = 60$ s; $\lambda = 407$ nm; $[KHSO_5] = 6 \times 10^{-3}$ M. Other experimental conditions: $[Fe^{III}(TPPS)] = 6 \times 10^{-6}$ M; pH 11; 25 °C; $I = 0.1$ M.

This can only be suppressed by working at a low $KHSO_5$ concentration, which then results in a slow redox cycle (reaction time *ca.* 1000 s). The proposed mechanism for the observed redox cycle is summarized in reactions (4) to (8) and is partly

$$(TPPS)Fe^{III}\text{–}O\text{–}Fe^{III}(TPPS) + SO_5^{2-} \longrightarrow (TPPS)Fe^{III}\text{–}O\text{–}Fe^{IV}(O)(TPPS^+) + SO_4^{2-} \quad (4)$$

$$2\{(TPPS)Fe^{III}\text{–}O\text{–}Fe^{IV}(O)(TPPS^+)\} \longrightarrow 2\{(TPPS)Fe^{III}\text{–}O\text{–}Fe^{III}(TPPS)\} + O_2 \quad (5)$$

$$(TPPS)Fe^{III}\text{–}O\text{–}Fe^{III}(TPPS) + SO_5^{2-} \longrightarrow \text{decomposition products} + SO_4^{2-} \quad (6)$$

$$(TPPS)Fe^{III}\text{–}O\text{–}Fe^{IV}(O)(TPPS^+) + SO_5^{2-} \longrightarrow \text{decomposition products} + SO_4^{2-} \quad (7)$$

$$HSO_5^- \rightleftharpoons H^+ + SO_5^{2-} \quad pK = 9.4 \quad (8)$$

Table 1 Fitted values, accuracies and confidence limits from the FACSIMILE fit of the experimental curves for the reaction between (TPPS)Fe^{III}-OFe^{III}(TPPS) and SO_5^{2-} (see Fig. 3)

Reaction	Value/M^{-1} s^{-1}	SDLN[a]	5% limit	95% limit	Suggested value
(4)	8.9581×10^3	0.0164	8.7192×10^3	9.2035×10^3	$(9.0 \pm 0.3) \times 10^3$
(5)	1.4381×10^3	0.0074	1.4206×10^3	1.4558×10^3	$(1.44 \pm 0.02) \times 10^3$
(7)	3.5046×10^1	0.0528	3.2132×10^1	3.8225×10^1	$(3.5 \pm 0.3) \times 10^1$
Not well determined values					
(6)	2.7045×10^1	0.3392	1.5478×10^1	4.7254×10^1	$(2.7 \pm 2.0) \times 10^1$

[a] Estimated standard deviation for the logarithm of each parameter value. The 5 and 95% limits indicate that there is a 5% probability that the true value lies below the lower limit, and a 95% probability that the true value lies below the upper limit.

based on reactions that form part of the suggested mechanism for the iron-catalysed autoxidation of sulfite.[13]

We suggest that during the redox cycle only one iron(III) centre of the Fe^{III}(TPPS) dimer is oxidized to Fe^{IV} by SO_5^{2-}. It is possible that this complex ((TPPS)$Fe^{III}OFe^{IV}$(O)($TPPS^+$)) can undergo rapid intramolecular charge rearrangement to result in the formation of (TPPS)$Fe^{IV}OFe^{IV}$(O)(TPPS),[28] but in the absence of any further evidence we prefer the former notation. Subsequently the back reaction takes place and O_2 is produced, eqn. (5). Since SO_5^{2-} is a strong oxidizing agent it is able to oxidize the TPPS ligand and to decompose the Fe^{III}(TPPS) dimer, eqn. (6). The same effect must also be considered for the (TPPS)$Fe^{III}OFe^{IV}$(O)($TPPS^+$) species, eqn. (7). Computer simulations based on reactions (4)–(8) using the FACSIMILE chemical modelling package[36] show good agreement between the experimental and simulated concentration profile (concentration *vs.* time curve; Fig. 3). In order to improve the accuracy, the rate constants were fitted simultaneously to the experimental curves at 405 (Fe^{III}(TPPS)) and 430 nm (Fe^{IV}(O)($TPPS^+$)). The rate constants obtained for reactions (4)–(7) are summarized in Table 1.

The rate constant obtained for reaction (4) (9×10^3 M^{-1} s^{-1}) is of the same magnitude as that reported[29] for the reaction of a ferrihaem dimer with HSO_5^- (5×10^3 M^{-1} s^{-1}). The rate constants from the simulation show that under the selected conditions the oxidation of Fe^{III}(TPPS) by $KHSO_5$ (reaction (4)) is about 6 times faster than the back reaction (reaction (5)). The rate constants for the decomposition of the complex by SO_5^{2-} (reactions (6) and (7)) are significantly smaller in comparison with the values obtained for the redox reactions. Therefore the redox cycle can be observed under the appropriate conditions. Since the data were fitted by the simplest possible reaction scheme that gives a good representation of the experimental curves a more detailed reaction scheme[29] cannot be ruled out.

Reaction of Fe^{III}(TPPS) with H_2O_2

Since it is known that iron porphyrins are oxidized by H_2O_2[30–32] similar experiments to those conducted for the reaction of Fe^{III}(TPPS) with $KHSO_5$ were performed with H_2O_2 in order to investigate if H_2O_2 (pK = 11.6) reacts in the same way as SO_5^{2-} and can induce a similar redox cycle. In agreement with earlier results using $KHSO_5$, the Fe^{III}(TPPS) monomer is also decomposed by H_2O_2 in an acidic medium (pH 3). The decomposition rate depends on the H_2O_2 concentration (the more H_2O_2, the faster the decomposition). The decomposition of the Fe^{III}(TPPS) dimer was also observed at pH 11 and at higher H_2O_2 concentrations ($[H_2O_2] = 4.4 \times 10^{-2}$ to 4.4×10^{-4} M). If the H_2O_2 concentration is decreased to 4.4×10^{-5} M then a redox cycle could be observed. First a portion of Fe^{III}(TPPS) was decomposed and then the redox cycle occurred (Fig. 4a). Obviously the H_2O_2 concentration (4.4×10^{-5} M) was still too high and therefore another experiment at even lower H_2O_2 concentration (4.4×10^{-6} M) was performed. The redox cycle is more clearly observed and does not involve the initial decomposition of Fe^{III}(TPPS) (Figs. 4b and 4c). The formation of the

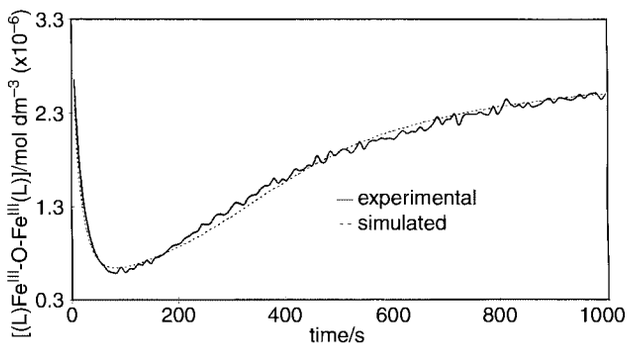

Fig. 3 Experimental and simulated concentration profile for the Fe^{III}-(TPPS) dimer for the redox cycle observed for Fe^{III}(TPPS) and $KHSO_5$. Simulated conditions: [Fe^{III}(TPPS) dimer] = 3×10^{-6} M; [$KHSO_5$] = 6×10^{-6} M; pH 11.

(TPPS)$Fe^{III}OFe^{IV}$(O)($TPPS^+$) band at 420 nm was fast (Fig. 4b) as compared to the slow back reaction (formation of (TPPS)-$Fe^{III}OFe^{III}$(TPPS) in Fig. 4c). The experiments with H_2O_2 clearly show that it is also able to induce a redox cycling of Fe^{III}(TPPS). The results are the same as for the reaction of Fe^{III}(TPPS) with $KHSO_5$; the redox cycle could only be observed at low H_2O_2 concentrations and at high pH where Fe^{III}(TPPS) exists as a dimer. At higher H_2O_2 concentrations only decomposition of the complex took place.

Redox cycling of Fe^{III}(TPPS) in the presence of sulfite and oxygen

Following the preliminary measurements described above for the reaction between Fe^{III}(TPPS) and sulfite on a long timescale during which no evidence for redox cycling was found, measurements on a much shorter timescale were performed. For this purpose we used a rapid scan spectrophotometric technique which coupled to a stopped-flow instrument enabled the recording of UV-VIS spectra on a millisecond timescale. In a typical experiment the total measurement time was 10.5 s and the cycle time between each consecutive spectrum was 42 ms, such that a total of 250 spectra were recorded. First the reaction of the Fe^{III}(TPPS) monomer with sulfite was investigated at pH 3. The recorded spectra showed that there were nearly no spectral changes on this relatively short timescale. However, the decomposition of Fe^{III}(TPPS) over a longer period of time, and the fact that oxygen is consumed during this time period, support the idea that a redox cycle similar to that outlined in reactions (1)–(3) operates during this period. The Fe^{II}(TPPS) concentration is most probable only too small to be observed spectrophotometrically due to the very effective back oxidation of Fe^{II}(TPPS) by $SO_5^{\bullet -}$.

The reaction of the Fe^{III}(TPPS) dimer with sulfite was studied at pH 11. First it was performed in nitrogen-saturated solutions and with a large excess of sulfite ([Fe^{III}(TPPS)] = 6×10^{-6} M; $[SO_3^{2-}] = 4 \times 10^{-4}$ M; I = 0.1 M). The recorded spectra also showed no spectral changes. If the experiment is

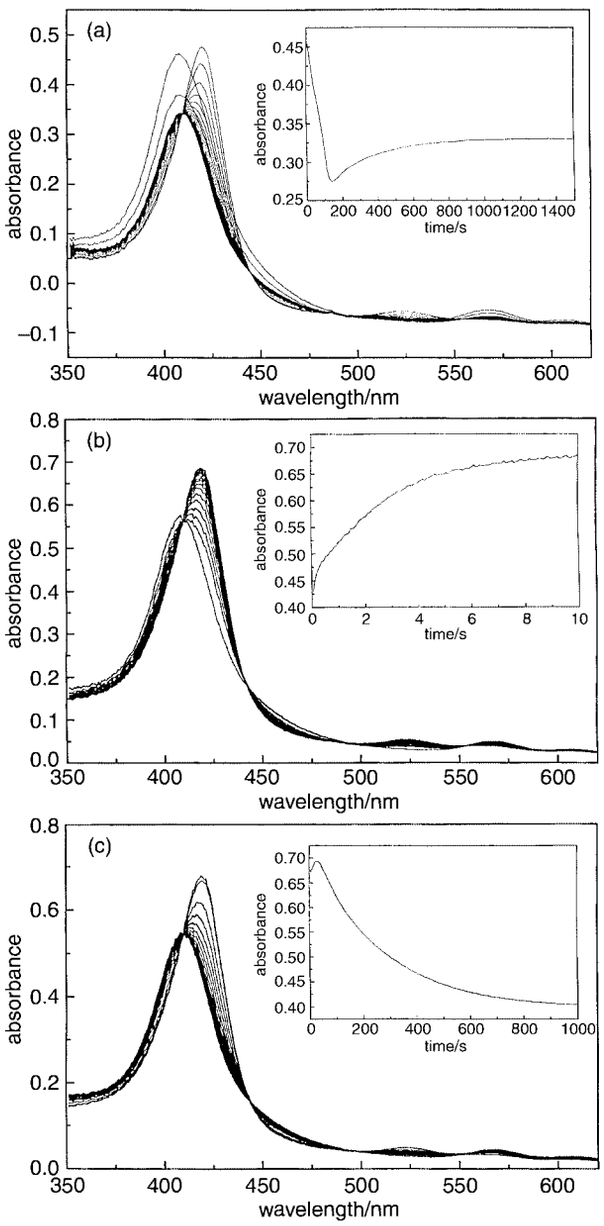

Fig. 4 (a) Spectral changes observed for the redox cycle between the Fe^{III}(TPPS) dimer and H_2O_2 in oxygen saturated solutions ($[H_2O_2] = 4.4 \times 10^{-5}$ M; $\Delta t = 60$ s). Insert: absorbance *vs.* time trace at $\lambda = 406$ nm. (b) Spectral changes observed for the formation of (TPPS)Fe^{III}–O–Fe^{IV}(O)($TPPS^+$) during the reaction between the Fe^{III}(TPPS) dimer and H_2O_2 in oxygen saturated solutions ($[H_2O_2] = 4.4 \times 10^{-6}$ M; $\Delta t = 0.6$ s). Insert: absorbance *vs.* time trace at $\lambda = 421$ nm. (c) Spectral changes observed for the back reaction of (TPPS)Fe^{III}–O–Fe^{IV}(O)($TPPS^+$) during the reaction between the Fe^{III}(TPPS) dimer and H_2O_2 in oxygen saturated solutions ($[H_2O_2] = 4.4 \times 10^{-6}$ M; $\Delta t = 60$ s). Insert: absorbance *vs.* time trace at $\lambda = 421$ nm. Other experimental conditions as in Fig. 2.

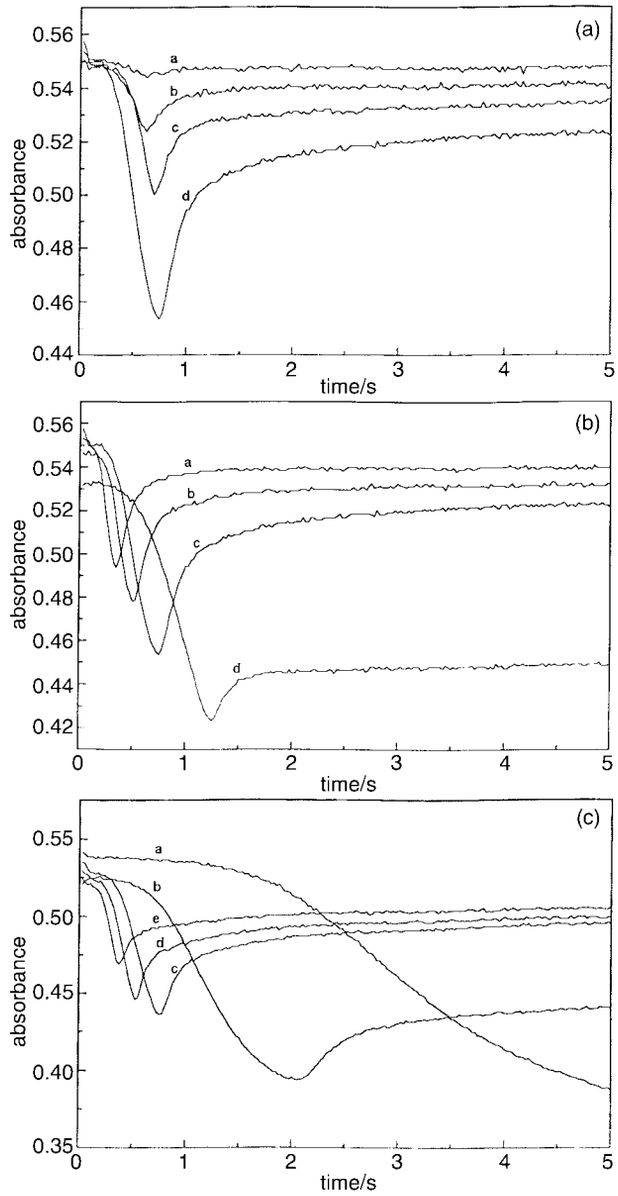

Fig. 5 Absorbance *vs.* time traces for the redox cycle between the Fe^{III}(TPPS) dimer and sulfite at $\lambda = 405$ nm (Fe^{III}(TPPS)) [Fe^{III}-(TPPS)] $= 6 \times 10^{-6}$ M, 25 °C and $I = 0.1$ M. (*a*) For different oxygen concentrations. Experimental conditions: $[S^{IV}] = 4 \times 10^{-3}$ M; pH 11; $[O_2] = 1.2 \times 10^{-4}$ (a), 2.4×10^{-4} (b), 6×10^{-4} (c) and 1.2×10^{-3} M (d). (*b*) In oxygen saturated solutions for different pH values. Experimental conditions: $[S^{IV}] = 4 \times 10^{-3}$ M; pH 9.2 (a), 10 (b), 11 (c) and 12 (d). (*c*) In oxygen saturated solutions for different sulfite concentrations. Experimental conditions: pH 11; $[S^{IV}] = 1 \times 10^{-3}$ (a), 2×10^{-3} (b), 4×10^{-3} (c), 6×10^{-3} (d) and 8×10^{-3} M (e).

repeated with air-saturated solutions, then the formation and disappearance of a shoulder at $\lambda \approx 426$ nm is observed (see Fig. 2, SUP 57588). Since the shoulder is very broad ($\lambda \approx 420$–428 nm) and the absorbance changes very small it is not possible to assign the appearance of this shoulder to the partial formation of either Fe^{II}(TPPS) or (TPPS)$Fe^{III}OFe^{IV}$(O)($TPPS^+$) due to the close similarity in their spectral properties in this wavelength range. The spectral changes and the absorbance *vs.* time traces indicate that a redox cycle does occur. The absorbance changes associated with this redox cycle are greatly enhanced when the reaction is repeated with oxygen-saturated solutions (see Fig 3a, SUP 57588). The formation and disappearance of a band at 420 nm can then clearly be seen. These spectral changes correspond to those observed for the reaction of Fe^{III}(TPPS) with $KHSO_5$ and with H_2O_2, which were attributed to the oxidation of (TPPS)$Fe^{III}OFe^{III}$(TPPS) to (TPPS)$Fe^{III}OFe^{IV}$(O)-($TPPS^+$). The absorbance *vs.* time traces at $\lambda = 430$ (to monitor Fe^{IV}(O)($TPPS^+$)) and 405 nm (to monitor Fe^{III}(TPPS)) nicely illustrate that a redox cycle occurs (see Fig. 3b, SUP 57588). After what looks like an induction period, the absorbance *vs.* time trace at $\lambda = 430$ nm first shows an increase due to the formation of Fe^{IV}(O)($TPPS^+$) and then a decrease due to the back reaction (reduction of Fe^{IV}(O)($TPPS^+$) to Fe^{III}(TPPS)), whereas the trace at $\lambda = 405$ nm shows the opposite trends.

The importance of oxygen for the observed redox cycle can be clearly seen in Fig. 5(*a*), which reports absorbance *vs.* time traces at $\lambda = 405$ ((TPPS)$Fe^{III}OFe^{III}$(TPPS)) and 430 nm ((TPPS)$Fe^{III}OFe^{IV}$(O)($TPPS^+$), see Fig. 4, SUP 57588) for different oxygen concentrations. A high oxygen concentration

results in large absorbance changes for the redox cycle. Thus oxygen induces the redox cycle due to the more effective formation of the different sulfur oxide radicals ($SO_5^{\bullet -}$, $SO_4^{\bullet -}$, *etc.*) which are responsible for the observed redox cycling. This is supported by the fact that in nitrogen-saturated solutions no redox cycling could be observed. The higher the oxygen concentration the more (TPPS)$Fe^{III}OFe^{IV}$(O)($TPPS^+$) is formed. It should also be taken into account that sulfur oxide radicals ($SO_5^{\bullet -}$, $SO_4^{\bullet -}$, *etc.*) are not only responsible for the redox cycling but also for the decomposition of Fe^{III}(TPPS) as observed during the measurements on a longer timescale. Therefore, in many cases the redox cycle back from (TPPS)$Fe^{III}OFe^{IV}$(O)-($TPPS^+$) to the Fe^{III}(TPPS) dimer does not proceed to 100% completion.

In all these cases a small induction period was observed before the redox cycle started. This indicates that certain reactions between Fe^{III}(TPPS) and sulfite/oxygen must take place before the observed redox cycle can be initiated, and involves the comsumption of oxygen due to the formation of the sulfur oxide radicals.

Exactly the same trends as decribed above were also observed in the longer wavelength range (450–650 nm) when the Fe^{III}-(TPPS) concentration was increased from 6×10^{-6} to 5×10^{-5} M in order to improve the observed spectral changes in this region. After what looked like an induction period, an increase followed by a decrease in a new absorption band at 525 nm was observed. This was accompanied by a decrease followed by an increase of the two characteristic absorption bands for Fe^{III}-(TPPS) at 570 and 620 nm. The overall redox cycle observed at these wavelengths looked very similar to that observed at 405 and 430 nm.

The redox cycle not only depends on the oxygen concentration, but also on pH and sulfite concentration. An increase in pH from 9 to 12 has a significant influence on the redox cycle as shown by the recorded absorbance *vs.* time traces in Fig. 5(b). The absorbance changes increase with increasing pH, which leads to the conclusion that more (TPPS)$Fe^{III}OFe^{IV}$(O)($TPPS^+$) is formed at higher pH. In addition, the time for the formation of (TPPS)$Fe^{III}OFe^{IV}$(O)($TPPS^+$) increases with increasing pH, thus the whole redox cycle (formation of (TPPS)$Fe^{III}OFe^{IV}$-(O)($TPPS^+$)) and back reduction to Fe^{III}(TPPS)) becomes slower at higher pH. At pH 12, where the redox cycle is slow, some decomposition also takes place. In general it can be concluded that a high pH value stabilizes the formation of (TPPS)$Fe^{III}OFe^{IV}$(O)($TPPS^+$) and therefore hinders the back reaction (*i.e.* reduction to Fe^{III}(TPPS)).

The sulfite concentration also has a significant influence on the observed redox cycle. The absorbance *vs.* time traces (Fig. 5c) show that if the sulfite concentration is decreased to 1×10^{-3} M the redox cycle is not complete due to partial decomposition. The complex (TPPS)$Fe^{III}OFe^{IV}$(O)($TPPS^+$) is formed and then slowly decomposed so that no back reduction to Fe^{III}(TPPS) takes place (Fig. 5c). If the sulfite concentraton is increased decomposition is hindered and the redox cycle becomes faster. This indicates that under strong oxidizing conditions (low sulfite concentration and high oxygen concentration), which results in a significant concentration of the sulfur oxide radicals ($SO_5^{\bullet -}$, $SO_4^{\bullet -}$, *etc.*), decomposition becomes more important since the radicals attack the TPPS ligand. At higher sulfite concentrations the side reactions of the sulfur oxide radicals with sulfite inhibit the decomposition of the ligand and therefore sulfite has a similar effect as a radical scavenger. This can also explain why the absorbance changes accompanying the redox cycle and the concentration of (TPPS)$Fe^{III}OFe^{IV}$(O)($TPPS^+$) become smaller on increasing the sulfite concentration. At high sulfite concentration the amount of sulfur oxide radicals (which are important for the redox cycle) is decreased due to the side reactions with sulfite.

In order to obtain further evidence for the participation of the sulfur oxide radicals in the redox cycling process alcohol-quenching studies were performed. It has been shown that $SO_4^{\bullet -}$ reacts rapidly with ethanol, whereas $SO_3^{\bullet -}$ and $SO_5^{\bullet -}$ both react 10^4 times slower.[33,34] Therefore the redox cycle could be affected by the addition of ethanol. It was performed at different ethanol concentrations (0.025 to 0.125 vol%) and the results were compared with the corresponding experiment in the absence of ethanol. A small amount of ethanol (0.025 vol%) inhibits the redox cycle (see Fig. 7, SUP 57588). The redox cycle is slower (50 instead of 10 s) and the absorbance changes during the cycle are also smaller, which means that less (TPPS)$Fe^{III}OFe^{IV}$(O)($TPPS^+$) is formed. A further increase in the ethanol concentration (0.05 vol%) leads to a further decrease in the absorbance changes; the band of (TPPS)Fe^{III}-OFe^{IV}(O)($TPPS^+$) appears only as a shoulder. If the ethanol concentration is increased to 0.125 vol% then no redox cycle is observed. In all alcohol quenching studies with Fe^{III}(TPPS) and sulfite a slow subsequent reaction takes place which gives rise to a new band at 415 nm accompanied by small absorbance changes. The ethanol dependence of the subsequent reaction suggests that ethanol does not only react with the sulfur oxide radicals but also with Fe^{III}(TPPS). The fact that ethanol inhibits the redox cycle demonstrates the important role of the sulfur oxide radicals (especially $SO_4^{\bullet -}$) in the redox cycling.

As in the case for the Fe^{III}(TPPS)–$KHSO_5$ system, we suggest a mechanism for the redox cycling of the Fe^{III}(TPPS)–sulfite–oxygen system which is based on reactions that participate in the suggested mechanism for the iron-catalysed autoxidation of sulfite.[13] In contrast to the Fe^{III}(TPPS)–$KHSO_5$ system, oxygen plays a significant role in the redox cycle of Fe^{III}(TPPS) with sulfite. This fact has to be considered in the proposed mechanism, eqns. (2), (4)–(7), (9)–(18).

$$(TPPS)Fe^{III}\text{–}O\text{–}Fe^{III}(TPPS) + SO_3^{2-} \rightleftharpoons (TPPS)Fe^{III}\text{–}O\text{–}Fe^{II}(TPPS) + SO_3^{\bullet -} \quad K = 7.8 \times 10^{-7} \quad (9)$$

$$SO_3^{\bullet -} + O_2 \longrightarrow SO_5^{\bullet -} \quad 2.5 \times 10^9\ M^{-1}\ s^{-1} \quad (2)$$

$$SO_5^{\bullet -} + SO_3^{2-} \longrightarrow SO_5^{2-} + SO_3^{\bullet -} \quad 1.05 \times 10^7\ M^{-1}\ s^{-1} \quad (10)$$

$$SO_5^{\bullet -} + SO_3^{2-} \longrightarrow SO_4^{2-} + SO_4^{\bullet -} \quad 7.5 \times 10^4\ M^{-1}\ s^{-1} \quad (11)$$

$$(TPPS)Fe^{III}\text{–}O\text{–}Fe^{II}(TPPS) + SO_5^{\bullet -} \longrightarrow (TPPS)Fe^{III}\text{–}O\text{–}Fe^{III}(TPPS) + SO_5^{2-} \quad (12)$$

$$SO_5^{2-} + SO_3^{2-} \longrightarrow SO_4^{2-} + SO_4^{2-} \quad 3.5 \times 10^2\ M^{-1}\ s^{-1} \quad (13)$$

$$(TPPS)Fe^{III}\text{–}O\text{–}Fe^{III}(TPPS) + SO_5^{2-} \longrightarrow (TPPS)Fe^{III}\text{–}O\text{–}Fe^{IV}(O)(TPPS^+) + SO_4^{2-} \quad (4)$$

$$SO_4^{\bullet -} + SO_3^{2-} \longrightarrow SO_4^{2-} + SO_3^{\bullet -} \quad 3.8 \times 10^8\ M^{-1}\ s^{-1} \quad (14)$$

$$(TPPS)Fe^{III}\text{–}O\text{–}Fe^{II}(TPPS) + SO_4^{\bullet -} \longrightarrow (TPPS)Fe^{III}\text{–}O\text{–}Fe^{III}(TPPS) + SO_4^{2-} \quad (15)$$

$$(TPPS)Fe^{III}\text{–}O\text{–}Fe^{III}(TPPS) + SO_5^{2-} \longrightarrow \text{decomposition products} + SO_4^{2-} \quad (6)$$

$$(TPPS)Fe^{III}\text{–}O\text{–}Fe^{IV}(O)(TPPS^+) + SO_3^{\bullet -} \longrightarrow (TPPS)Fe^{III}\text{–}O\text{–}Fe^{III}(TPPS) + SO_4^{\bullet -} \quad (16)$$

$$(TPPS)Fe^{III}\text{–}O\text{–}Fe^{IV}(O)(TPPS^+) + SO_5^{2-} \longrightarrow \text{decomposition products} + SO_4^{2-} \quad (7)$$

$$(TPPS)Fe^{III}\text{–}O\text{–}Fe^{IV}(O)(TPPS^+) + (TPPS)Fe^{III}\text{–}O\text{–}Fe^{II}(TPPS) + H^+ \longrightarrow 2\{(TPPS)Fe^{III}\text{–}O\text{–}Fe^{III}(TPPS)\} + HO^{\bullet} \quad (17)$$

Table 2 Fitted values, accuracies and confidence limits from the FACSIMILE fit of the experimental curves for the reaction between (TPPS)Fe^{III}O-Fe^{III}(TPPS) and SO_3^{2-} (see Fig. 6)

Reaction	Value/M^{-1} s^{-1}	SDLN[a]	5% lmiit	95% limit	Suggested value
Well determined values					
(9) (forward)	8.6856	0.0080	8.5717	8.8010	8.69 ± 0.12
(9) (backward)	1.1148×10^7	0.0927	9.5709×10^6	1.2985×10^7	$(1.1 \pm 0.2) \times 10^7$
(16)	1.3788×10^8	0.0363	1.2988×10^8	1.4636×10^8	$(1.38 \pm 0.09) \times 10^8$
(4)	6.1999×10^3	0.0130	6.0685×10^3	6.3341×10^3	$(6.2 \pm 0.2) \times 10^3$
(17)	3.5537×10^{14}	0.1450	2.7994×10^{14}	4.5114×10^{14}	$(3.6 \pm 1.0) \times 10^{14}$
(6)	2.3193×10^2	0.0122	2.2733×10^2	2.3662×10^2	$(2.32 \pm 0.05) \times 10^2$
Not well determined values					
(12)	4.72×10^5	1.1162	5.3256×10^4	2.0955×10^6	4.7×10^5
(7)	8.45	2.4490	3.9265×10^{-2}	1.2395×10^2	8.5×10^2
Data do not determine values					
(15)	8.41×10^8				8.4×10^8
(5)	1.27×10^3				1.3×10^3

[a] Estimated standard deviation for the logarithm of each parameter value. The 5 and 95% limits indicate that there is a 5% probability that the true value lies below the lower limit, and a 95% probability that the true value lies below the upper limit.

$$2\{(TPPS)Fe^{III}\text{–}O\text{–}Fe^{IV}(O)(TPPS^+)\} \longrightarrow 2\{(TPPS)Fe^{III}\text{–}O\text{–}Fe^{III}(TPPS)\} + O_2 \quad (5)$$

$$SO_3^{2-} + HO^{\bullet} \longrightarrow SO_3^{\bullet -} + OH^- \quad 4.6 \times 10^9\ M^{-1}\ s^{-1} \quad (18)$$

The rate constants given in the reaction scheme are taken from the literature[5,12,13,35] and used in the simulations as fixed values. In the above mechanism the formation of the sulfite radical (reaction (9)) and its subsequent fast reaction (2) with oxygen to the peroxomonosulfate radical play a significant role in the multiple redox cycling ($Fe^{III}/Fe^{II}/Fe^{IV}$) of the Fe^{III}(TPPS)–sulfite–oxygen system. In nitrogen saturated solutions no spectral changes were observed. For the redox cycle of the Fe^{III}-(TPPS) with sulfite, the presence of oxygen is absolutely necessary and an induction period clearly occurred. In the case of the Fe^{III}(TPPS)–$KHSO_5$ system no oxygen dependence and no induction period were observed, indicating that in the observed redox cycle with sulfite the oxidizing species (peroxomonosulfate/peroxomonosulfate radical) first have to be formed in order to initiate the Fe^{III}/Fe^{IV} redox cycle. First a portion of the Fe^{III}(TPPS) is reduced by sulfite and a sulfite radical is formed (reaction (9)). The sulfite radical reacts rapidly with the oxygen present in solution to the peroxomonosulfate radical (reaction (2)) which is able to oxidize sulfite or Fe^{II}(TPPS) (reactions (10) and (12)). In both reactions peroxomonosulfate is formed which, as in the case of the Fe^{III}(TPPS)–$KHSO_5$ system, oxidizes Fe^{III}(TPPS) to Fe^{IV}(TPPS) (reaction (4)) or oxidizes the TPPS ligand leading to the decomposition of the complex (reactions (6) and (7)). The back reaction of Fe^{IV} to Fe^{III} occurs through the sulfite radical (reaction (16)), through the proton catalysed redox reaction between Fe^{IV} and Fe^{II} (reaction (17)), and through the redox reaction between two iron(IV) species (reaction (5)). In addition, it should be taken into consideration that sulfur oxides or sulfur oxide radicals not only react with the metal complex but also with the excess of sulfite in solution (reactions (10), (11), (13) and (14)). The sulfite itself thereby reacts as a kind of radical scavenger. The same effect also occurs for the $HO^{\bullet}$ radicals (reaction (18)). Computer simulations based on the reactions (2), (4)–(7), (9)–(18) using the FACSIMILE chemical modelling package show good agreement between the experimental and simulated concentration profiles (concentration *vs.* time curves in Fig. 6). The values for the varied rate constants are summarized in Table 2. It is important to note that the reported values were obtained from many simulations over a wide sulfite and oxygen concentration range. Although the data do not determine the values of all the rate constants under the specific conditions, they do under other conditions. It is therefore obvious that the accuracies and confidence limits vary under different conditions.

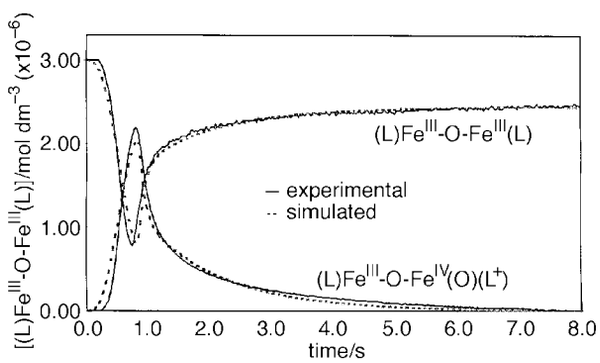

Fig. 6 Experimental and simulated concentration profile for the Fe^{III}-(TPPS) dimer and (TPPS)$Fe^{III}OFe^{IV}$(O)($TPPS^+$) during the redox cycle observed for Fe^{III}(TPPS) and sulfite in oxygen saturated solutions. Simulated conditions: [Fe^{III}(TPPS) dimer] = 3×10^{-6} M; [S^{IV}] = 4×10^{-3} M; pH 11.

The rate constants clearly show that under the selected conditions the formation of the peroxomonosulfate radical (reaction (2)) and of peroxomonosulfate (reaction (10)) is very fast. Both species play a significant role and initiate the second (Fe^{III}/Fe^{IV}) redox cycle between the Fe^{III}(TPPS) dimer and sulfite. The peroxomonosulfate produced in the Fe^{III}(TPPS)–sulfite–oxygen system reacts in the same way as in the proposed mechanism for the Fe^{III}(TPPS)–$KHSO_5$ system (reactions (4) to (8)). The rate constants obtained from the simulation for these reactions approximately agree within the experimental and evaluation error limits with those obtained from the simulation of the redox cycle between Fe^{III}(TPPS) and $KHSO_5$. Theoretically the k values for these reactions should be identical in both simulations. Since concentration *vs.* time profiles are preferred for the simulations with the FACSIMILE program, a transformation of the experimental obtained absorbance *vs.* time traces to concentration *vs.* time traces is necessary. This transformation is associated with some difficulties and thus with some errors since the absorbance changes associated with the redox cycle are small and the absorbance bands or maxima of the different Fe(TPPS) species partly overlap. Concentration curves for (TPPS)$Fe^{III}OFe^{III}$(TPPS) and (TPPS)$Fe^{III}OFe^{IV}$(O)($TPPS^+$) were calculated by using the molar absorptivity values for these complexes at 405 and 430 nm, respectively (*e.g.* $\approx 1.1 \times 10^5$ and $\approx 8 \times 10^4$ M^{-1} cm^{-1}). The corresponding minimum molar absorptivity values at these wavelengths are subtracted from these values. The maximum absorbance changes at these

wavelengths can then be related to the maximum concentration (3×10^{-6} M) of the dimeric species. In addition, it should be taken into consideration that during the redox cycle several parallel reactions take place which are responsible for the observed absorbance changes. The back reaction of Fe^{IV} to Fe^{III} occurs according to the results of the simulation, through the sulfite radical (reaction (16)), through the proton catalysed redox reaction between Fe^{IV} and Fe^{II} (reaction (17)) and through the redox reaction between two iron(IV) species (reaction (5)). Thus in the case of the Fe^{III}(TPPS)–sulfite–oxygen system the back reaction and therefore the complete redox cycle is much faster (only a few seconds) than in the case of the Fe^{III}(TPPS)–$KHSO_5$ system (*ca.* 1000 s).

On the basis of the proposed mechanism the sulfite and the oxygen concentration dependence of the multiple redox cycles for the Fe^{III}(TPPS)–sulfite–oxygen system were simulated by using the FACSIMILE program (Fig. 7(a) and 7(b)). The simulated concentration *vs.* time curves in Fig. 7(b) show that at low sulfite concentration (1×10^{-3} M) the Fe^{III}/Fe^{IV} redox cycle is not complete because of interfering decomposition. The complex (TPPS)$Fe^{III}OFe^{IV}$(O)($TPPS^+$) is formed and then slowly decomposed so that no back reduction to Fe^{III}(TPPS) occurs (Fig. 7(b)). If the sulfite concentration is increased the decomposition is inhibited and the redox cycle becomes faster. The simulation results for the sulfite dependence are in good agreement with the experimentally obtained sulfite dependence for the Fe^{III}(TPPS)–sulfite–oxygen system (see Fig. 5(c)). The simulated concentration *vs.* time curves in Fig. 7(a) clearly show the influence of oxygen on the redox cycle. The higher the oxygen concentration the larger are the observed concentration changes for the observed redox cycle. The reason is that at high oxygen concentrations more $SO_5^{\bullet -}$ is formed, which leads to the formation of SO_5^{2-} that initiates the Fe^{III}/Fe^{IV} redox cycle. This redox cycle is therefore hardly observed at low oxygen concentrations. The simulation results are in good agreement with the experimentally obtained oxygen dependence of the Fe^{III}(TPPS)–sulfite–oxygen system (see Fig. 5(b)).

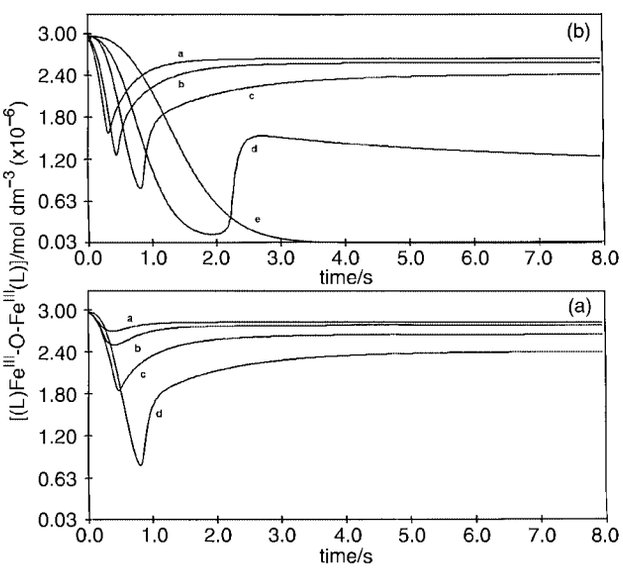

Fig. 7 Simulated concentration profiles for the Fe^{III}(TPPS) dimer during the redox cycle observed for Fe^{III}(TPPS) and sulfite, [Fe^{III}(TPPS) dimer] = 3×10^{-6} M, pH 11, $T = 25$ °C, $I = 0.1$ M. (*a*) At different oxygen concentrations. Simulated conditions: $[S^{IV}] = 4 \times 10^{-3}$ M; $[O_2] = 1 \times 10^{-4}$ (a), 2×10^{-4} (b), 5×10^{-4} (c) and $[O_2] = 1 \times 10^{-3}$ M (d). (*b*) In oxygen saturated solutions at different sulfite concentrations. Simulated conditions: $[S^{IV}] = 8 \times 10^{-3}$ (a), 6×10^{-3} (b), 4×10^{-3} (c), 2×10^{-3} (d) and 1×10^{-3} M (e).

In Fig. 8 the simulated concentration *vs.* time curves for the most important species involved in the redox cycle of the Fe^{III}(TPPS)–sulfite–oxygen system are presented. The calculated curves clearly demonstrate the opposite concentration trends of the two Fe(TPPS) species. The concentration of the Fe^{III}(TPPS) dimer decreases because of the formation of the (TPPS)$Fe^{III}OFe^{IV}$(O)($TPPS^+$) by peroxomonosulfate. Subsequently, the back reaction takes place to the Fe^{III}(TPPS) dimer. Beside the redox reactions also decomposition reactions occur, with the result that the redox cycle is not 100% complete. Since the reaction of the sulfite radical with oxygen to form the peroxomonosulfate radical is very efficient, the oxygen concentration nearly decreases to zero. The peroxomonosulfate radical reacts rapidly with the excess of sulfite to form further sulfur oxides (sulfate, peroxomonosulfate) and sulfur oxide radicals (sulfite and sulfate radicals). Thus the concentration of these species increases. The peroxomonosulfate concentration decreases after some time since it is used up during the decomposition reactions with the two Fe(TPPS) species. The sulfite concentration decreases during the redox cycle since it reacts with the sulfur oxides and the sulfur oxide radicals. In comparison with the other species, the decrease in the sulfite concentration is not so significant since it is present in large excess.

Taking the complexity of the system into account, the results obtained from the computer simulations are in good agreement with the experimental results. The concentration *vs.* time profiles of the Fe^{III}/Fe^{IV} redox cycle as well as the sulfite and the oxygen dependence could be successfully simulated on the basis of the proposed mechanism. It should, however, be noted that the proposed mechanism, which is partly based on the suggested mechanism of the iron-catalysed autoxidation of sulfite,[13] can only approximately describe the very complex Fe^{III}(TPPS)–sulfite–oxygen system. Many known[5] reactions of the sulfur species, but probably less important for this system, were not included in the model. The suggested reaction scheme is also incomplete in that no acid–base equilibria have been taken into account. Many more reaction steps and equilibrium data will be necessary to simulate the pH dependence of the

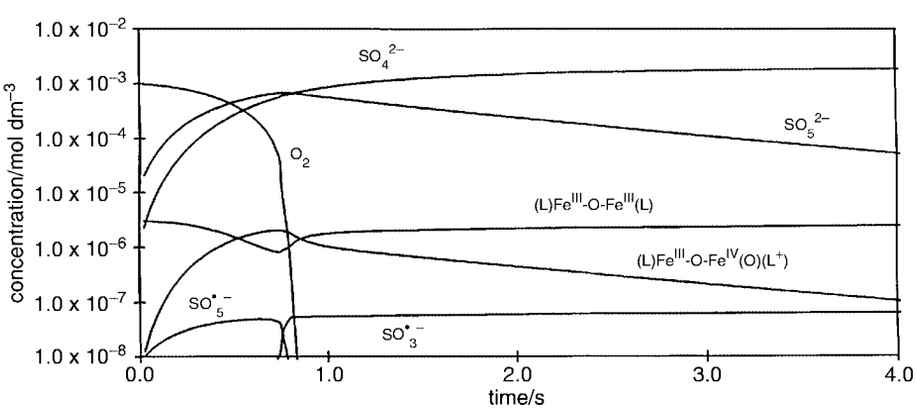

Fig. 8 Simulated concentration profiles for some important species involved in the redox cycle between Fe^{III}(TPPS) and sulfite. Simulated conditions: [Fe^{III}(TPPS) dimer] = 3×10^{-6} M; $[S^{IV}] = 4 \times 10^{-3}$ M; $[O_2] = 1 \times 10^{-3}$ M; pH 11.

reaction. There is, however, no doubt that it gives a very good description of the observed experimental trends under the selected conditions.

Conclusion

The results of this study have clearly revealed the conditions under which Fe^{III}(TPPS) can be oxidized to Fe^{IV}(O)($TPPS^{+}$), decomposition of Fe^{III}(TPPS) takes place, or a redox cycle between the Fe^{III}(TPPS) dimer and (TPPS)$Fe^{III}OFe^{IV}$(O)-($TPPS^{+}$) occurs. Under strong oxidizing conditions various strong oxidants such as $SO_5^{\bullet -}$, HSO_5^{-} and H_2O_2 can cause a decomposition of Fe(TPPS), which presumably involves the oxidation to Fe^{III}($TPPS^{+}$) followed by decomposition of the TPPS chelate. Oxidation of Fe^{III}(TPPS) to Fe^{IV}(O)($TPPS^{+}$) is more favourable at high pH in the presence of sulfite, where the concentration ratios of Fe(TPPS), sulfite and dissolved oxygen are very critical for the stabilization of Fe^{IV}(O)($TPPS^{+}$). The latter species can react with sulfite radicals ($SO_3^{\bullet -}$) and peroxomonosulfate back to Fe^{III}(TPPS), at which stage the remaining oxidizing power will determine the extent of further oxidation of Fe^{III}(TPPS) that will be accompanied by the decomposition of TPPS.

Our earlier work on the redox cycling of Fe^{II}/Fe^{III} in the presence of sulfite and oxygen clearly showed that $SO_4^{\bullet -}$, HSO_5^{-} and $SO_5^{\bullet -}$ are responsible for the rapid oxidation of Fe^{II} to Fe^{III}. Our present results show that the Fe^{III}/Fe^{II} redox cycle can be close to 100% efficient under well controlled experimental conditions, involving pH, sulfite and oxygen concentration. In addition, such a redox cycle can occur on a short timescale (a couple of seconds), such that conventional kinetic techniques are not suitable to detect such a redox cycling process. This redox cycling will form the basis of a catalysed autoxidation of sulfite, and could under well selected conditions lead to a very efficient catalytic system. The multiple redox cycles observed in the current system are quite unique and only observed for the Fe^{III}(TPPS) dimer. This is probably related to the stability of the (TPPS)$Fe^{III}OFe^{IV}$(O)($TPPS^{+}$) dimer under the selected conditions. As a result of the μ-oxo bridge in the Fe^{III}(TPPS) dimer, the axially co-ordinated water molecules are expected to be extremely labile, and could in this way favour the interaction with peroxomonosulfate to produce the Fe^{IV}(O)-($TPPS^{+}$) species, something that will be less likely in the case of the monomeric species.

Acknowledgements

The authors gratefully acknowledge financial support from the Fonds der Chemischen Industrie, Deutsche Forschungsgemeinschaft, the Volkswagen Foundation, the Foundation for Reseach Development (SA), Eskom Technology Group and Eskom Human Resources. They kindly acknowledge the help of Professor Dr J. Daub, University of Regensburg, with the spectroelectrochemical measurements.

References

1 K. M. Smith, *Porphyrins and Metalloporphyrins*, Elsevier, Amsterdam, 1975; D. Dolphin, *The Porphyrins*, Academic Press, New York, 1978.
2 A. P. Hong, D. W. Bahnemann and M. R. Hoffmann, *J. Phys. Chem.*, 1987, **91**, 6245.
3 B. Meunier, *Chem. Rev.*, 1992, **92**, 1411.
4 G. Behra and L. Sigg, *Nature* (*London*), 1990, **344**, 419.
5 C. Brandt and R. van Eldik, *Chem. Rev.*, 1995, **95**, 119 and refs. therein.
6 J. Kraft and R. van Eldik, *Inorg. Chem.*, 1989, **28**, 2297.
7 J. Kraft and R. van Eldik, *Inorg. Chem.*, 1989, **28**, 2306.
8 M. H. Conklin and M. R. Hoffmann, *Environ. Sci. Technol.*, 1988, **22**, 899.
9 K. Bal Reddy and R. van Eldik, *Atmos. Environ.*, 1992, **26A**, 661.
10 N. Coichev and R. van Eldik, *Inorg. Chem.*, 1991, **30**, 2375.
11 J. Berglund, S. Fronaeus and L. I. Elding, *Inorg. Chem.*, 1993, **32**, 4527.
12 C. Brandt, I. Fabian and R. van Eldik, *Inorg. Chem.*, 1994, **33**, 687.
13 P. Warneck, *Heterogeneous and Liquid-Phase Processes*, Springer, Heidelberg, 1996 and refs. therein.
14 M. A. Kline, M. H. Barley and T. J. Meyer, *Inorg. Chem.*, 1987, **26**, 2196.
15 S. M. Chen, *J. Electroanal. Chem. Interfacial Electrochem.*, 1996, **407**, 123.
16 K. Hatano, K. Usui and Y. Ishida, *Bull. Chem. Soc. Jpn.*, 1981, **54**, 413.
17 K. Hatano and Y. Ishida, *Bull. Chem. Soc. Jpn.*, 1982, **55**, 3333.
18 B. Welman, Ph.D. Thesis, Potchefstroom University, 1996.
19 K. Strachan, Master Thesis, Potchefstroom University, 1993.
20 E. B. Fleischer, J. M. Palmer, T. S. Srivastava and A. Chatterjee, *J. Am. Chem. Soc.*, 1971, **93**, 3162.
21 J. Salbeck, *Anal. Chem.*, 1993, **65**, 2169.
22 J. R. Sutter, P. Hambright, P. B. Chock and M. Krishnamurthy, *Inorg. Chem.*, 1974, **13**, 2764.
23 F. L. Harris and D. L. Toppen, *Inorg. Chem.*, 1978, **17**, 71.
24 A. A. El-Awady, P. C. Wilkins and R. G. Wilkins, *Inorg. Chem.*, 1985, **24**, 2053.
25 M. H. Barley, K. J. Takeuchi and T. J. Meyer, *J. Am. Chem. Soc.*, 1986, **108**, 5876.
26 N. Motohashi and Y. Saito, *Chem. Pharm. Bull.*, 1995, **43**, 505.
27 W. V. Steele and E. H. Appelman, *J. Chem. Thermodyn.*, 1982, **14**, 337.
28 S. E. J. Bell, P. R. Cooke, P. Inchley, D. R. Leanord, J. R. Lindsay Smith and A. Robbins, *J. Chem. Soc.*, *Perkin Trans. 2*, 1991, 549.
29 D. M. Davies and N. D. Gillitt, *J. Chem. Soc.*, *Dalton Trans.*, 1995, 3323.
30 M. F. Zipplies, W. A. Lee and T. C. Bruice, *J. Am. Chem. Soc.*, 1986, **108**, 4433.
31 R. Panicucci and T. C. Bruice, *J. Am. Chem. Soc.*, 1990, **112**, 6063.
32 T. G. Traylor and F. Xu, *J. Am. Chem. Soc.*, 1990, **112**, 178.
33 P. Neta and R. E. Huie, *Environ. Health Perspect.*, 1985, **64**, 209.
34 P. Neta, R. E. Huie and A. B. Ross, *J. Phys. Chem. Ref. Data*, 1988, **17**, 1027.
35 G. V. Buxton, S. McGowan, J. E. Williams and N. D. Wood, *Atmos. Environ.*, 1996, **30A**, 2483.
36 FACSIMILE chemical modelling package, AEA Technology, Harwell, Oxfordshire, UK, 1994.

Paper 9/02746G